13th U. S. National Combustion Meeting
Organized by the Central States Section of the Combustion Institute
March 19–22, 2023
College Station, Texas

The Effect of Porosity on Flexoelectricity in Fluoropolymer/Aluminum Films

Thomas A. Hafner[1], Metin Örnek[1], Diane N. Collard[1], Derek K. Messer[1], Cohen T. Nunes[2], Mark W. Paral[2], Steven F. Son[1]*

[1] School of Mechanical Engineering, Purdue University, West Lafayette, Indiana 47907, USA
[2] School of Aeronautical and Astronautical Engineering, Purdue University, West Lafayette, Indiana 47907, USA
[*]Corresponding Author Email: thafner@purdue.edu

Abstract: In this study, the effect of porosity and aluminum content on flexoelectricity for fluoropolymer/aluminum films was investigated. Specifically, samples with different size scales (thin and thick films), manufacturing methods (tape casting and 3-D printing), fluoropolymers (polyvinylidene fluoride (PVDF) and polyvinylidene fluoride trifluoroethylene (P(VDF-TrFE)), and aluminum sizes (micrometers and nanometers) were fabricated and tested. Measurements of the flexoelectric constant for nAl/PVDF and nAl/P(VDF-TrFE) were conducted for the first time. We found that decreasing porosity (increasing infill) increased the average flexoelectric coefficient. Also, adding aluminum to the fluoropolymer increased the average flexoelectric coefficient for all except one set of samples. These results indicate that the charge generation due to flexoelectricity can be altered by changing material/sample parameters, which may be utilized to sensitize energetic materials.
Keywords: Flexoelectricity, Porosity, Fluoropolymer, Aluminum

1. Introduction

Flexoelectricity is a topic of recent interest in the research community due to its potential applications in sensors, actuators, energy generation, energy harvesting and more [1]. Flexoelectricity is defined as the mechanical-electro coupling between strain gradient and electric polarization [1]. It is similar to piezoelectricity (mechanical-electro coupling between strain and electric polarization) except for the difference of strain gradient and uniform strain. Equation one defines the change of polarization in a material as a combination of the piezoelectric and flexoelectric effects,

$$\Delta P_i = e_{ijk}\varepsilon_{jk} + \mu_{ijkl}\frac{\partial \varepsilon_{jk}}{\partial x_l}, \tag{1}$$

where ΔP_i is the change in polarization, $e_{ijk}\varepsilon_{jk}$ is the piezoelectric contribution and $\mu_{ijkl}\frac{\partial \varepsilon_{jk}}{\partial x_l}$ is the flexoelectric contribution [2]. Flexoelectricity can be present in centrosymmetric materials, unlike piezoelectric materials, and is not limited by working temperature [1]. Additionally, flexoelectricity in nano scale applications is of note relative to its piezoelectric counterpart. This is due to strain gradient scaling with thinner samples.

Shu et al. [1] documented three direct measurement methods for quantifying the flexoelectric coefficient: cantilever beam, bottom-up side of truncated pyramid and lateral side of truncated pyramid. These three methods are used to measure the transverse, longitudinal and shear flexoelectric coefficient, respectively [1]. Four literature reviews summarize the literature on flexoelectricity [1,3–5]. Shu et al. [1], Zubko et al. [4], and Wang et al. [5] tabulated previous experimental data on the flexoelectric coefficient measured for a wide variety of different materials.

Poddar et al. [2] examined flexoelectricity by casting a thin film onto a glass slide. The slide was then bent as a cantilever beam. Following this, the flexoelectric coefficient was determined through the resulting current output and known displacement profile using theoretical relationships derived in the paper. Chu et al. [6] used a hot-press manufacturing method to produce thick film samples of polymers. A cantilever beam setup was then used to measure the flexoelectric coefficient with one sample end fixed and the other moved via shaker. Using measured current off the sample and the known displacement profile, the flexoelectric coefficient was calculated using a derived relationship between the applied strain and the output electrical signals. Zaitzeff et al. [7] used the cantilever beam setup to study the effect of manufacturing method (fused filament fabrication 3-D printing, direct ink write 3-D printing, and casting) and solids loading of aluminum on the flexoelectric effect of THV (tetrafluorethylene, hexafluorpropylene and vinylidenfluoride)/aluminum and PVDF/aluminum composites. The flexoelectric coefficient of PVDF has been measured to be between 0.7025 – 15.24 nC/m [6–15] with an occasional larger measurement [16–19]. The flexoelectric coefficient of P(VDF-TrFE) has been measured to as between 3.04 – 191 nC/m [2,20]. The flexoelectric coefficient of μAl/PVDF was measured by Zaitzeff et al. [7] to be between 5.66 and 6.52 nC/m. Prior to this work, the flexoelectric coefficient of nAl/PVDF and nAl/P(VDF-TrFE) had never been measured.

Zaitzeff et al. [7] claims based on the work of Zhang et al. [21] and Zhao et al. [22] that porosity induces strain gradients which contribute to the overall flexoelectric effect. Also, Beni [23] notes that increasing porosity increases the electrical polarization for the direct flexoelectric effect state. However, Shu et al. [24] found in his study that porosity weakens the flexoelectric effect. Additionally, Hahn [25] reported that porosity degraded the flexoelectric coefficients of materials in his study. The objective of this work is to investigate the effect of porosity (infill) and addition of aluminum particles on the flexoelectric coefficient of fluoropolymer/aluminum films.

2. Methods / Experimental

This study employs the cantilever beam method in order to measure the transverse flexoelectric coefficient (μ_{12}) of materials. Two sizes of samples (thick and thin films) were employed. The thick films (2 mm thickness) were oscillated in the bending cantilever scheme while the thin films (10 μm - 100 μm thickness) were tape casted onto a substrate which was oscillated. The thin film experimental methods were based on the work of Poddar et al. [2] and the thick films experimental methods were based on the work of Zaitzeff et al. [7] and Chu et al. [6].

The fluoropolymers used were P(VDF-TrFE) (70/30 mol ratio, Arkema) and PVDF (Kynar 711, Arkema). The aluminum (nAl, Novacentrix) nanopowders (50 – 80 nm diameter) have 70 wt. % active content as determined by differential scanning calorimetry and thermogravimetric analysis (DSC/TGA). The micron aluminum (Skylighter Inc) was ~5 μm in diameter. The solvents used were dimethylformamide (DMF, Fisher Chemical) and Acetone (Reagents). The PVDF printing filament was purchased from 3DXTECH. Electrically conductive tape (3M) was used as electrodes and microscope cover glasses (24 mm x 50 mm x 0.17 mm) were used as substrates upon which the thin film samples were cast.

The thick films were printed on two different printers: Hyrel 3D SR printer and Ender 3 V2 3D printer. For the Ender, the bed and nozzle temperatures were 95 ˚C and 245 ˚C, respectively. The prints were done using PVDF (3DXTECH) filament that was 1.75 mm in diameter. The thick films have dimensions of 21.25 mm x 67 mm x 2 mm. The porosity of the film was controlled by setting the infill at different values from 10% to 100%. The samples at 10%, 20%, 40% used a cubic infill pattern whereas the samples at 60%, 80% and 100% infill used the line infill pattern.

The bed and nozzle temperatures were 70 ˚C and 240 ˚C, respectively, for printing using the Hyrel printer. The PVDF filament was purchased from 3DXTECH whereas the μAl/PVDF and nAl/PVDF printing filament was prepared in the lab. The in-lab materials were prepared by mixing DMF, acetone, fluoropolymer, and aluminum powder at a ratio of 7 mL (2mL DMF and 5mL Acetone) solvent to 1 g of solid material. Following this, a vortex mixer (Fisher Scientific) was used to break up clumps of solid material in the solution. Next, an ultrasonic mixer (Branson) was utilized in order to completely mix the solution. Following this, the mixture was cast into aluminum tins and allowed time for the solvent to evaporate. After evaporation was complete, the material was chopped up into approximately 2 mm x 2 mm x 2 mm chunks by hand. This chopped material was then extruded into 3D printer filament using a filament extruder (Filabot). The μAl/PVDF and nAl/PVDF samples were both 28.6 wt. % Al. The samples all had a rectilinear infill pattern.

To prepare the substrate for tape casting, electrically conductive tape was placed on top of the glass slides. Following this, we mixed the DMF, fluoropolymer and aluminum additives (if included) at a ratio of 6 mL solvent to 1 g of solid material. A vortex mixer (Fisher Scientific) was then used to break up clumps of solid material in the solution. Next, an ultrasonic mixer (Branson) was utilized in order to completely mix the solution. After the solution was well mixed, a tape caster (MSK-AFA-HC100, MIT) was employed to cast thin films on top of the substrate. For the porous solutions, the tape caster bed temperature was 60 ˚C and for the full density solutions, the tape caster bed was 100 ˚C. This difference in bed temperature caused the difference in porosity. The sample thicknesses were between 10 - 80 μm. The nAl/P(VDF-TrFE) films were 20 wt.% nAl. Figure 1 is a schematic of this process.

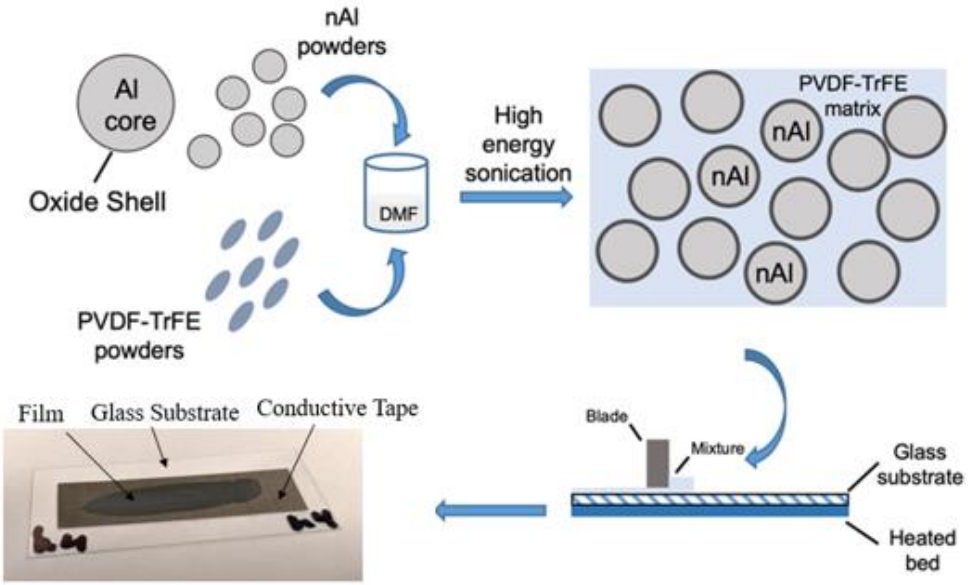

Figure 1: The schematic of the film fabrication process [26]

Density and porosity measurements were done using the Archimedes tests. Scanning electron microscopy (SEM) imaging was performed at 5 kV on several thin film samples to investigate the microstructure and illustrate the difference between full density and porous thin films using a FEI Nova NanoSEM. Prior to imaging, the films were sputter-coated with 10 nm of palladium and platin alloy to create a conductive layer on the sample's surface.

For thick films, Salem and Chu [6] gave an equation relating current and beam deflection,

$$i = \frac{2\pi f \mu'_{12} b L}{x^2\left(1 - {}^{x}/_{3L}\right)} w(x). \tag{2}$$

We can set x = L and obtain

$$i = \frac{3\pi f \mu'_{12} b}{L} w(L). \tag{3}$$

A schematic of the measurement setup can be seen in Fig. 2. A diagram of the bending film can be observed in Fig. 3. The setup is the same for the thick and thin films, but the theoretical equations differ. The electromagnetic shaker bends the film by actuating up and down while the other end of the film is fixed. While this is happening, the accelerometer measures the acceleration of the shaker in real-time. We can use an equation to relate this acceleration value to deflection (w(L)),

$$w(L) = \frac{a}{(2\pi f)^2}. \tag{4}$$

The lock-in amplifier measures the current (i) coming off of the film. The frequency of the electromagnetic shaker needs to be equal to the frequency of the reference signal inputted into

the lock-in amplifier. The frequency used in this study was 10 Hz. The lock-in amplifier displays its current reading as a voltage value that can be converted back into current using the following equation:

$$i = \text{sensitivity}\frac{V}{10V}. \tag{5}$$

The dimensions of the film (b, L) are measured with a pair of calipers. After the measurements were made, the current is plotted against the deflection and the slope of the line is equal to $\frac{3\pi f \mu'_{12} b}{L}$. From there, we can solve for the flexoelectric coefficient (μ'_{12}).

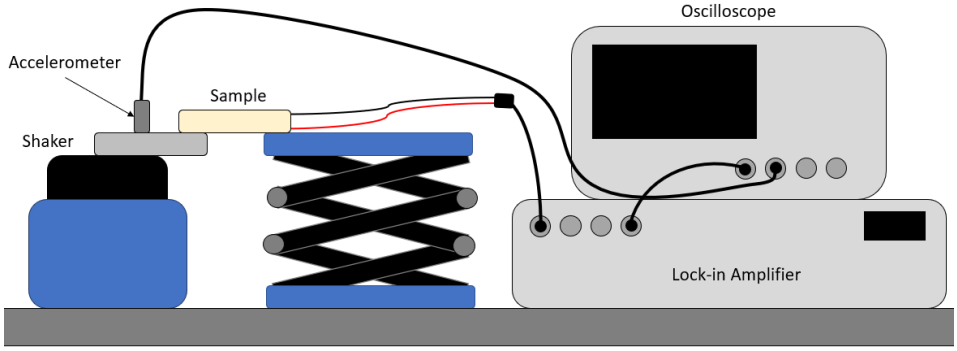

Figure 2: Schematic of flexoelectric measurement setup

For thin films, Poddar et al. [2] gave an equation relating the change in polarization ($\Delta P = \frac{J}{2\pi fA}$) to strain gradient ($\varepsilon' = \frac{c}{L^2}$),

$$\frac{J}{2\pi fA} = \mu_{12}\frac{c}{L^2}. \tag{6}$$

The length of the substrate and electrode area are found via calipers. The current (J) and deflection (c) are found in the same manner outlined previously. After collecting data, $\frac{J}{2\pi fA}$ was plotted versus $\frac{c}{L^2}$ with the slope being the flexoelectric coefficient (μ_{12}).

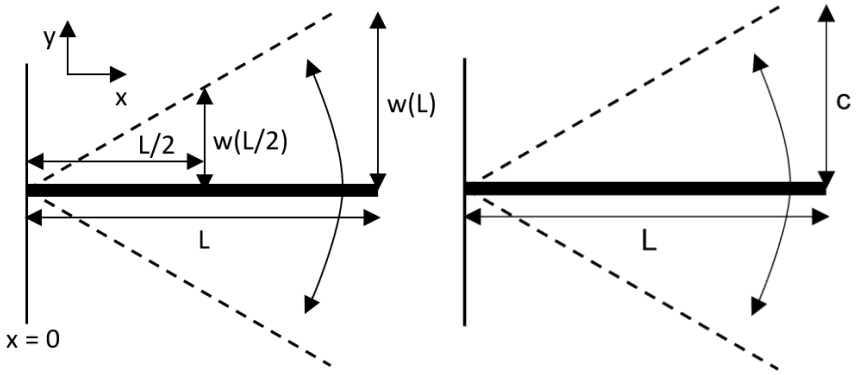

Figure 3: Diagram of the bending thick film (left) and thin film (right)

3. Results and Discussion

Figure 4 displays the SEM images taken on a porous nAl/P(VDF-TrFE) thin film (left) and a full density nAl/P(VDF-TrFE) thin film (right). The cross-section image on the porous film shows some defects such as pores and uneven surfaces, whereas the full density film has a solid cross-section surface with no visible pores.

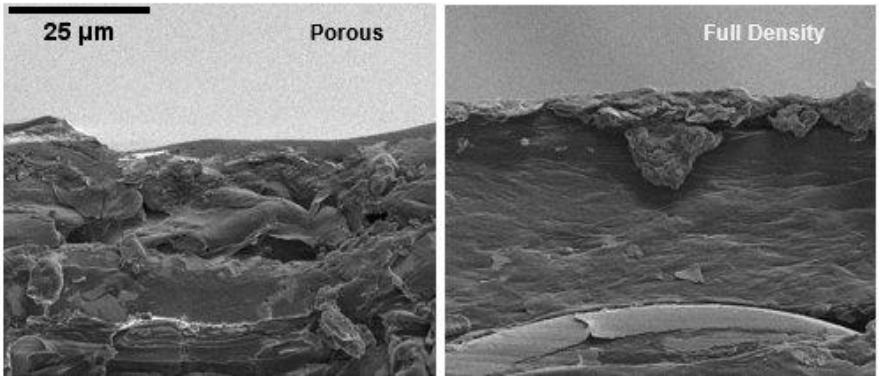

Figure 4: SEM images of nAl/P(VDF-TrFE) thin films

Figure 5 illustrates the effect of porosity on flexoelectricity for 3D printed (Ender) PVDF films. All of our PVDF measurements are in the typical range from the literature [6–15]. Near full-density thick films have flexoelectric coefficient of μ_{12} = 2.760 nC/m. With increasing the porosity up to 10%, a sharp decrease in the flexoelectric coefficient to ~ 0.5 nC/m was observed. The higher porosity levels above 10% did not change the relatively lower values of the flexoelectric coefficient, which varied between ~ 0.5-1 nC/m.

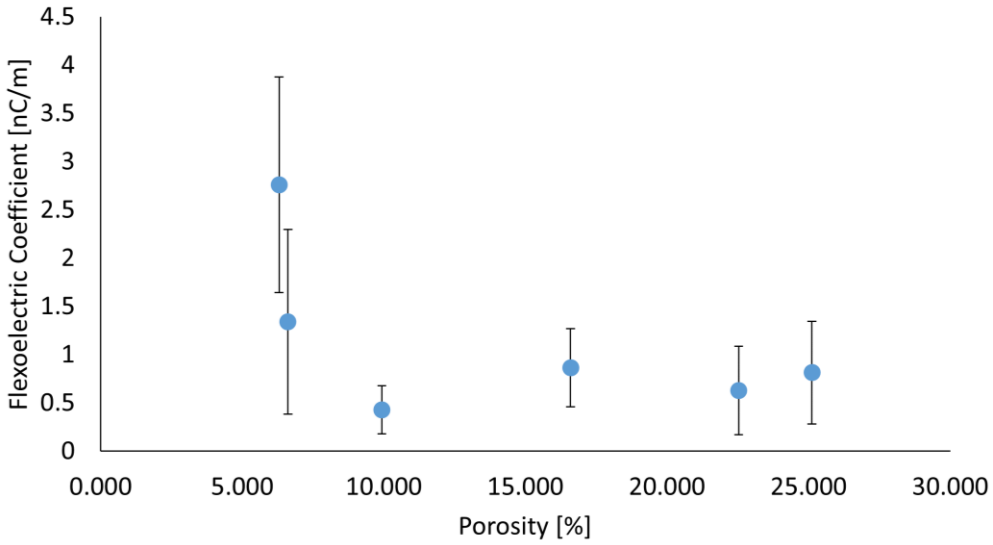

Figure 5: Flexoelectric coefficient as a function of porosity for PVDF (Ender 3D printed films)

Figure 6 displays the effect of infill percent and aluminum addition on flexoelectricity for 3D printed (Hyrel) films. The literature values for PVDF [6–15] and µAl/PVDF [7] are comparable to the values measured. The nAl/PVDF flexoelectric coefficient was measured to be 8.017 and 10 nC/m for the 10% and 100% infill samples, respectively. For the printed low-infill (higher

porosity) samples, neat PVDF and μAl/PVDF samples show μ_{12} of ~3 nC/m. While the addition of the micron particles to the PVDF matrix does not seem to result in any significant difference in flexoelectric coefficient at high porosity levels, on the other hand, the addition of Al nanoparticles resulted in higher μ_{12} value. This may be attributed to, in addition to the engineered porosities within the sample created by 3D printing, the incorporation of smaller porosities in nanometer size scales caused by nanoparticle agglomeration within the PVDF matrix [27]. The effect of smaller porosities on flexoelectricity was investigated by Zhang et al. [21] which will further be discussed later. Conversely, for near full-density films of the same material systems, slightly higher μ_{12} values were observed for the printed μAl/PVDF film as compared to nAl/PVDF and neat PVDF samples, which is in accord with Zaitzeff et al. [7]. This might be attributed to higher strain gradients caused by larger particles and larger particle/polymer interface compared to nanosized aluminum at the same amount of displacement/bending of the sample. We note that the standard deviation is relatively high for μAl/PVDF 100% infill.

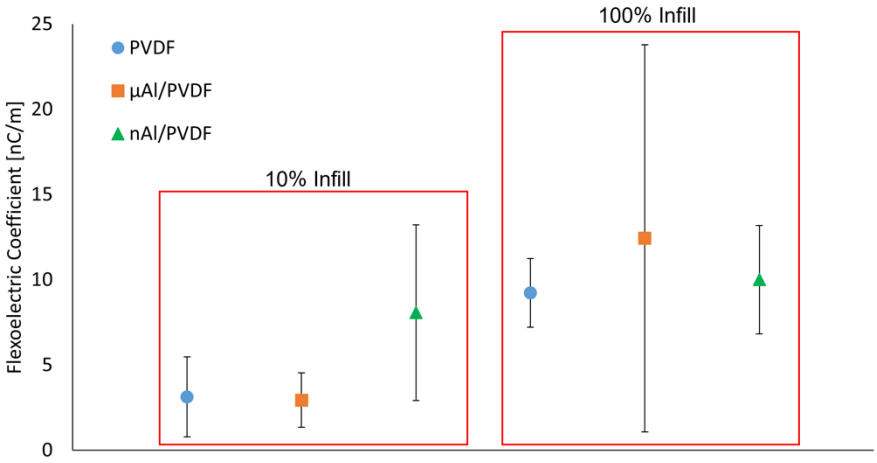

Figure 6: Flexoelectric coefficient for PVDF and nAl/PVDF at 10% and 100% infill (Hyrel 3D printed films)

We also investigated the effect of porosity and aluminum on flexoelectricity for P(VDF-TrFE) and nAl/P(VDF-TrFE) thin films fabricated by tape casting, and the test results of these materials systems are summarized in Figure 7. The values found for P(VDF-TrFE) are comparable to values in the literature [2,20]. The flexoelectric coefficient of nAl/P(VDF-TrFE) was measured to be 49.04 and 43.486 nC/m for full density and porous films respectively. The addition of aluminum nanoparticles increases the flexoelectric coefficient of the thin films regardless of incorporated porosity or density, which aligns with Zaitzeff et al. [7]. We note that the flexoelectric coefficient of the thin films are 2 to 3 times larger than their thick PVDF counterpart. This may be attributed to different chemical and materials property of P(VDF-TrFE), where a 30% mol ratio of TrFE changes specific material properties such as density, elastic modulus, etc., which in return may affect the level of polarization or strain gradient caused by the same amount of deflection in the beam.

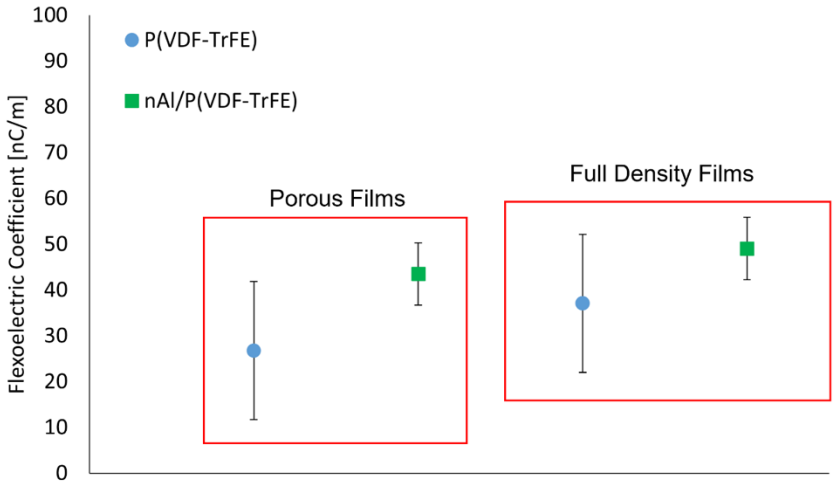

Figure 7: Flexoelectric coefficient values for full density and porous thin films

Overall, the results show that decreasing porosity (increasing infill) of thick and thin films increases the average flexoelectric coefficient for all three data sets. Our results are in accord with Shu et al. [24], and Hahn [25], where it is found that higher porosity levels decrease the flexoelectric coefficients of their samples. However, it must be mentioned that Zaitzeff et al. [7], Zhang et al [21], Zhao et al [22], and Beni [23] reported the opposite trend: higher porosity leads to larger flexoelectricity levels.

Zhang et al. [21] found flexoelectricity to be inversely related to the average size of pores of a porous film. Zaitzeff et al. [7] stated that large pores (millimeter scale) may have a negligible contribution to the overall flexoelectric coefficient compared to smaller pores (micron scale). This may explain the phenomena we observed in our tests, where 100% infill (near full density, low porosity) films may have had smaller pores size than the 10% infill (high porosity), causing the average flexoelectric coefficient to be higher, especially for samples with nanosized aluminum. Essentially, it is possible that for higher flexoelectricity levels, you may want porosity but with small (micrometer scale) pores and not large (millimeter scale) pores. Additionally, it can be noted that adding aluminum to P(VDF-TrFE) and PVDF increased the average flexoelectric coefficient in all but one case for PVDF, which is in accord with the results published by Zaitzeff et al. [7].

4. Conclusions

Flexoelectric measurements were made on fluoropolymer/aluminum films to study the effect of porosity (infill) and aluminum on flexoelectricity. It was found in all three data sets that decreasing porosity (increasing infill) increases the average flexoelectric coefficient. This trend matches the work of two authors in the literature [24,25] but contradicts the work of four [7,21–23]. One potential explanation for the observed phenomenon is that the high infill (low porosity) films had smaller pores than the low infill (high porosity) films. This explanation is based on work that showed that size of pore is inversely related to contribution to flexoelectricity [21]. We also found that adding aluminum increased the average flexoelectric coefficient for all but one case which matches trends from previous work [7]. The flexoelectric measurements on nAl/PVDF and nAl/P(VDF-TrFE) were done for the first time. Overall, our work helps further

understand the relationship between flexoelectricity and porosity for energetic fluoropolymer/aluminum films.

5. Acknowledgements

This research was sponsored by the Air Force Office of Scientific Research Award No: FA9550-19-1-0008 (Program Manager: Dr. Mitat Birkan). Any opinions, findings, conclusions, or recommendations expressed in the article are those of the authors and do not necessarily reflect the views of the United States Air Force.

6. References

[1] L. Shu, R. Liang, Z. Rao, L. Fei, S. Ke, Y. Wang, Flexoelectric materials and their related applications: A focused review, J. Adv. Ceram. 8 (2019) 153–173.
[2] S. Poddar, S. Ducharme, Measurement of the flexoelectric response in ferroelectric and relaxor polymer thin films, Appl. Phys. Lett. 103 (2013) 1–6.
[3] T.D. Nguyen, S. Mao, Y.W. Yeh, P.K. Purohit, M.C. McAlpine, Nanoscale flexoelectricity, Adv. Mater. 25 (2013) 946–974.
[4] P. Zubko, G. Catalan, A.K. Tagantsev, Flexoelectric effect in solids, Annu. Rev. Mater. Res. 43 (2013) 387–421.
[5] B. Wang, Y. Gu, S. Zhang, L.Q. Chen, Flexoelectricity in solids: Progress, challenges, and perspectives, Prog. Mater. Sci. 106 (2019).
[6] B. Chu, D.R. Salem, Flexoelectricity in several thermoplastic and thermosetting polymers, Appl. Phys. Lett. 101 (2012) 1–4.
[7] M.J. Zaitzeff, L.J. Groven, Flexoelectricity in fluoropolymer/aluminium reactives, Polym. Int. (2021).
[8] Y. Zhou, J. Liu, X. Hu, B. Chu, S. Chen, D. Salem, Flexoelectric effect in PVDF-based polymers, IEEE Trans. Dielectr. Electr. Insul. 24 (2017) 727–731.
[9] Y. Zhou, J. Liu, X. Hu, D.R. Salem, B. Chu, Apparent piezoelectric response from the bending of non-poled PVDF, Appl. Phys. Express. 12 (2019).
[10] X. Hu, Y. Zhou, J. Liu, B. Chu, Improved flexoelectricity in PVDF/barium strontium titanate (BST) nanocomposites, J. Appl. Phys. 123 (2018).
[11] J. Lu, J. Lv, X. Liang, M. Xu, S. Shen, Improved approach to measure the direct flexoelectric coefficient of bulk polyvinylidene fluoride, J. Appl. Phys. 119 (2016).
[12] S. Zhang, M. Xu, G. Ma, X. Liang, S. Shen, Experimental method research on transverse flexoelectric response of poly(vinylidene fluoride), Jpn. J. Appl. Phys. 55 (2016).
[13] S. Zhang, M. Xu, X. Liang, S. Shen, Shear flexoelectric coefficient μin polyvinylidene fluoride, J. Appl. Phys. 117 (2015).
[14] T. Hu, L. Chen, W. Mao, Atomistic modeling of flexoelectricity in amorphous polymers, J. Mol. Graph. Model. 92 (2019) 147–153.
[15] S. Zhang, X. Liang, M. Xu, B. Feng, S. Shen, Shear flexoelectric response along 3121 direction in polyvinylidene fluoride, Appl. Phys. Lett. 107 (2015).
[16] S. Baskaran, X. He, Q. Chen, J.Y. Fu, Experimental studies on the direct flexoelectric effect in α -phase polyvinylidene fluoride films, Appl. Phys. Lett. 98 (2011) 1–4.
[17] S. Baskaran, X. He, Y. Wang, J.Y. Fu, Strain gradient induced electric polarization in -phase polyvinylidene fluoride films under bending conditions, J. Appl. Phys. 111 (2012).
[18] J. Lu, J. Wu, X. Li, Measurement of Flexoelectric Response in Polyvinylidene Fluoride Beam, Lect. Notes Electr. Eng. 880 LNEE (2022) 739–746.

[19] S. Baskaran, N. Ramachandran, X. He, S. Thiruvannamalai, H.J. Lee, H. Heo, Q. Chen, J.Y. Fu, Giant flexoelectricity in polyvinylidene fluoride films, Phys. Lett. Sect. A Gen. At. Solid State Phys. 375 (2011) 2082–2084.
[20] J. Liu, Y. Zhou, X. Hu, B. Chu, Flexoelectric effect in PVDF-based copolymers and terpolymers, Appl. Phys. Lett. 232901 (2018).
[21] M. Zhang, D. Yan, J. Wang, L.H. Shao, Ultrahigh flexoelectric effect of 3D interconnected porous polymers: modelling and verification, J. Mech. Phys. Solids. 151 (2021).
[22] X. Zhao, S. Zheng, Z. Li, Effects of porosity and flexoelectricity on static bending and free vibration of AFG piezoelectric nanobeams, Thin-Walled Struct. 151 (2020) 106754.
[23] Y. Tadi Beni, Size dependent coupled electromechanical torsional analysis of porous FG flexoelectric micro/nanotubes, Mech. Syst. Signal Process. 178 (2022) 109281.
[24] L. Shu, Z. Yong, X. Jiang, Z. Xie, W. Huang, Flexoelectricity in low densification materials and its implication, J. Alloys Compd. 695 (2017) 1555–1560.
[25] M. Hahn, Flexoelectricity in the barium strontium titanate (bst) system for hydrophones, 2020.
[26] D. Messer, T. Hafner, M. Örnek, M. Paral, S.F. Son, Piezo-Energetic composite film fabrication and poling process for pressure sensor applications, Int. Pyrotech. Soc. (2022)
[27] M. Örnek, K.E. Uhlenhake, Y. Zhou, B. Zhang, M. Kalaswad, D.N. Collard, H. Wang, Q. Wang, S.F. Son, Preparation and characterization of multifunctional piezoenergetic polyvinylidene fluoride/aluminum nanocomposite films, J. Appl. Phys. 131 (2022) 055108.